The Natural Naphthoquinone Plumbagin Exhibits Antiproliferative Activity and Disrupts the Microtubule Network through Tubulin Binding†

Bipul R. Acharya,‡ Bhabatarak Bhattacharyya,§ and Gopal Chakrabarti*,‡

Dr. B. C. Guha Centre for Genetic Engineering and Biotechnology, University of Calcutta, 35 Ballygunge Circular Road, Kolkata, WB 700019, India, and Department of Biochemistry, Bose Institute, Kolkata, WB 700054, India

Received January 30, 2008; Revised Manuscript Received May 29, 2008

ABSTRACT: Plumbagin (5-hydroxy-2-methyl-1,4-naphthoquinone), a naphthoquinone isolated from the roots of *Plumbaginaceae* plants, has potential antiproliferative activity against several tumor types. We have examined the effects of plumbagin on cellular microtubules *ex vivo* as well as its binding with purified tubulin and microtubules *in vitro*. Cell viability experiments using human non-small lung epithelium carcinoma cells (A549) indicated that the IC_{50} value for plumbagin is 14.6 μM. Immunofluorescence studies using an antitubulin FITC conjugated antibody showed a significant perturbation of the interphase microtubule network in a dose dependent manner. *In vitro* polymerization of purified tubulin into microtubules is inhibited by plumbagin with an IC_{50} value of 38 ± 0.5 μM. Its binding to tubulin quenches protein tryptophan fluorescence in a time and concentration dependent manner. Binding of plumbagin to tubulin is slow, taking 60 min for equilibration at 25 °C. The association reaction kinetics is biphasic in nature, and the association rate constants for fast and slow phases are 235.12 ± 36 M^{-1} s^{-1} and 11.63 ± 11 M^{-1} s^{-1} at 25 °C respectively. The stoichiometry of plumbagin binding to tubulin is 1:1 (mole:mole) with a dissociation constant of 0.936 ± 0.71 μM at 25 °C. Plumbagin competes for the colchicine binding site with a K_i of 7.5 μM as determined from a modified Dixon plot. Based on these data we conclude that plumbagin recognizes the colchicine binding site to tubulin. Further study is necessary to locate the pharmacophoric point of attachment of the inhibitor to the colchicine binding site of tubulin.

Plumbagin (5-hydroxy-2-methyl-1,4-naphthoquinone), a naturally occurring yellow pigment, is found in the root of *Plumbaginaceae* plants (*1*). It has been used in Indian traditional medicine for more than 2500 years and possesses antiatherosclerotic (*2*), antiparasitic (*3*), antimicrobial (*4, 5*), and antioxidant properties (*5*). Plumbagin has also been shown to exert anticancer and antiproliferative activities in animal models as well as in cells in culture (*6–13*). It exhibits an inhibitory effect on carcinogenesis in the intestines and significantly inhibited azoxymethane-induced intestinal carcinogenesis in rats, suggesting its chemopreventive activity (*7*). Plumbagin causes cytogenetic and cell cycle changes in mouse Ehrlich ascites carcinoma, and possesses antiproliferative activity in human cervical cancer cells (*7, 8*). It induces G_2/M cell cycle arrest through the induction of p21 (an inhibitor of cyclin-dependent kinase) (*10–12*). Recent reports showed that plumbagin has chemotherapeutic potential as an anticancer agent in ovarian cancer cells possessing a mutant *BRCA1* gene (*8*) and also suppresses the NF-*k*B activation (*13*).

Microtubules are dynamic polymers composed of the tubulin heterodimer (α and β) subunits. They perform a variety of cellular functions, including mitosis, cell division, cell motility, maintenance of cell shape and structure, cell signaling, and organelle transport (*14–18*). Normal cell division requires proper construction of the mitotic spindle apparatus, and microtubule dynamics play a critical role during the formation and function of this spindle apparatus. The tubulin−microtubule equilibrium in a cell has been a very popular target for anticancer drug development; such drugs bind either tubulin or the microtubule and affect the dynamicity of microtubules (*19*). While paclitaxel and vinblastine are two widely used drugs employed for treating different types of cancer, many natural products target either tubulin or microtubules and are in different stages of drug development (*20–30*).

So far, all studies with plumbagin reported either *in vivo* or *ex vivo* conditions. There has been no report of plumbagin binding to purified protein *in vitro*. In this study, we examined the binding activity of plumbagin with tubulin and microtubules. We found that *in vitro* plumbagin binds to tubulin at the colchicine binding site, quenches tryptophan fluorescence and inhibits microtubule polymerization. We also studied the *ex vivo* perturbation of interphase microtubules in human non-small lung epithelial cancer cells (A549) and found that microtubule perturbation correlates well with the antimitotic activity of plumbagin. Our results demonstrate the novel activity of plumbagin that it inhibits cell proliferation and induces cell killing is by disruption of cellular

† The work was supported by grants from CSIR, Government of India (No.37(1216)/05/EMR-II) and BRNS/DAE, Government of India (No. 2006/37/21/BRNS) to G.C.

* Correspondence to Gopal Chakrabarti, Dr. B. C. Guha Centre for Genetic Engineering and Biotechnology, University of Calcutta, 35 Ballygunge Circular Road, Kolkata, WB 700019, India. Tel: 91-33-2461-4983. Fax: 91-33-2461-4849. E-mail: gcbcg@caluniv.ac.in.

‡ University of Calcutta.

§ Bose Institute.

10.1021/bi800730q CCC: $40.75
Published on Web 07/03/2008

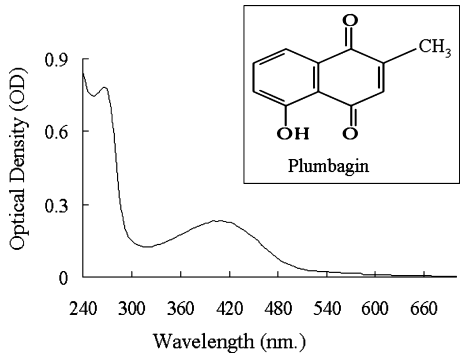

FIGURE 1: The absorption spectrum of 50 μM plumbagin, and the inset shows the chemical structure of plumbagin (5-hydroxy-2-methyl-1,4-naphthoquinone).

microtubules through tubulin binding. Thus, plumbagin alone or in combination with other antimicrotubule agents may be evaluated for its clinical potential against several types of cancers.

EXPERIMENTAL PROCEDURES

Materials. Nutrient mixture F12 Ham (supplemented with 1 mM L-glutamine), fetal bovine serum, penicillin-streptomycin and amphotericin B were purchased from HyClone, USA; Trypsin-Versene was purchased from Cambrex Bioscience, USA; and plumbagin, DAPI,[1] FITC conjugated monoclonal anti-α-tubulin antibody (raised in mouse), guanosine 5′-triphosphate (GTP), PIPES, $MgCl_2$, and EGTA were purchased from SIGMA, USA. The Bradford Protein estimation kit was from Genei, India. All other chemicals and reagents were local products of analytical grade.

Purification of Tubulin from Goat Brain. Microtubular proteins were isolated from goat brain by two cycles of a temperature-dependent assembly and disassembly process. Pure tubulin was isolated from microtubular proteins by two additional cycles of temperature-dependent polymerization−depolymerization using 1 M glutamate buffer for assembly (*31*). All experiments were performed in PEM buffer (50 mM PIPES, pH 6.9, 1 mM EGTA, 0.5 mM $MgCl_2$) unless otherwise mentioned. Aliquots were flash-frozen in liquid nitrogen and stored at −70 °C. The protein concentration was estimated by the method of Bradford (*32*) using bovine serum albumin as the standard.

Preparation of Plumbagin Solution. Plumbagin (molecular weight: 188.18), 1 mg of dry powder by weight, was directly dissolved in 100% DMSO (total volume 1 mL). The molar extinction coefficient (ϵ) was calculated from the absorption spectrum of 50 μM plumbagin in PEM buffer as shown in Figure 1. The molar extinction coefficient was 4590.6 ± 1.16 M^{-1} cm^{-1} ($P < 0.02$) at 410 nm and 15634.10 ± 0.76 M^{-1} cm^{-1} ($P < 0.01$) at 265 nm respectively. Concentration of plumbagin was calculated using molar extinction coefficient 4590 M^{-1} cm^{-1} at 410 nm. All experiments were done preparing secondary solutions in PEM buffer where final DMSO concentration was less than 1%.

Cell Culture. Human lung epithelial carcinoma cells (A549) were maintained in the nutrient mixture F12 Ham supplemented with 1 mM L-glutamine, 10% fetal bovine serum, 50 μg/mL penicillin, 50 μg/mL streptomycin and 2.5 μg/mL amphotericin B. Cells were cultured at 37 °C in a humidified atmosphere containing 5% CO_2. Cells were grown in tissue culture flasks until they were 80% confluent before trypsinization with 1 × Trypsin-Versene and splitting. Normal and treated cell morphology was observed and brightfield images were taken by Olympus inverted microscope model CKX41.

Cell Proliferation Inhibition Assay (MTT Assay). Inhibition of cell proliferation by plumbagin was measured by MTT (3-(4, 5-dimethylthiazolyl-2)-2,5-diphenyltetrazolium bromide) assay. Cells were plated in 96-well culture plates (1×10^4 cells per well). After 24 h incubation, the cells were treated with plumbagin (0, 5, 10, 20, 30 and 50 μM) for 12 h. MTT (5 mg/mL) dissolved in PBS and filter sterilized, then 20 μL of the prepared solution was added to each well. This was incubated until purple precipitate was visible. Subsequently 100 μL of Triton-X was added and incubated in the well under darkness for 2 h at room temperature. The absorbance was measured on an ELISA reader (Multiskan EX, Labsystems, Helsinki, Finland) at a test wavelength of 570 nm and a reference wavelength of 650 nm. Data were calculated as the percentage of inhibition by the following formula:

$$\% \text{ inhibition} = [100 - (A_t/A_s) \times 100]\% \quad (1)$$

where A_t and A_s indicate the absorbance of the test substances and solvent control, respectively (*12*).

Sample Preparation for Confocal Microscopy. Human lung epithelial carcinoma cells (A549) were seeded on coverslips at a density of 1×10^5 cells/mL and incubated in the presence of different doses of plumbagin (0− 50 μM) for 3 h. Plumbagin containing medium was then removed, and the cells were washed twice with PBS and fixed by incubation in 2% paraformaldehyde at room temperature for 1 h. Cell permeable solution (0.1% Na-citrate, 0.1% Triton) was added, and cells were incubated at room temperature for 1 h. Nonspecific binding sites were blocked by incubating the cells with 5% BSA in PBS overnight at 4 °C. Cells were then incubated with mouse monoclonal antibody-FITC conjugated (antimouse IgG) to α-tubulin (1:100 dilution) and DAPI to nucleus (1:1000 dilution of 1 mg/mL stock solution) for 2 h at 37 °C. After incubation, cells were washed twice with PBS and pictures were taken using a Ziess LSM 510 Meta confocal microscope.

Microtubule Polymerization. Tubulin (1.2 mg/mL) was mixed with different concentrations of plumbagin (0−85 μM) and incubated for 60 min at 25 °C. Polymerization reaction was initiated by incubating the tubulin−plumbagin complex in polymerization buffer (1 mM $MgSO_4$, 1 mM EGTA, 1.0 M monosodium glutamate, pH 6.8) at 37 °C adding 1 mM GTP in the assembly. Tubulin polymerization reaction was monitored by light scattering at 350 nm using a V-630 Jasco spectrophotometer (*33*).

Transmission Electron Microscopy. Tubulin (1.2 mg/mL) was polymerized at 37 °C in the absence and presence of plumbagin, for 60 min. Microtubules were then fixed in 0.5% prewarmed glutaraldehyde for 5 min. Each sample (10 μL) was loaded on carbon-coated electron microscope grids (300-mesh) for 20 s and blotted dry. The grids were subsequently negatively stained with 1% uranyl acetate and air-dried. The

[1] Abbreviation: PIPES, 1,4-piperazinediethanesulfonic acid; EGTA, ethylenebis(oxyethylenenitrilo)tetraacetic acid; GTP, guanosine 5′-triphosphate; DAPI, 4′,6-diamidino-2-phenylindole; FITC, fluorescein isothiocyanate; AC, (2-methoxy-5-(2′,3′,4′-trimethoxyphenyl)-tropone).

samples were viewed using a Philips Fei Technai Spirit electron microscope. Images were taken at 63000× magnifications (*30*).

Binding Measurements by Fluorescence Spectroscopy. All fluorescence measurements were performed using a Hitachi fluorescence spectrophotometer model F-3010 equipped with a constant temperature water-circulating bath. A 1 cm path length quartz cuvette was used for all fluorescence measurements. Quenching of tryptophan fluorescence of tubulin upon plumabagin binding was used to calculate several binding parameters of tubulin plumbagin interactions. Fluorescence data was corrected for the inner filter effect according to equation of Lakowicz (*34*),

$$F_{corr} = F_{obs}\ \text{antilog}[(A_{ex} + A_{em})/2] \quad (2)$$

where A_{ex} is the absorbance at the excitation wavelength and A_{em} is the absorbance at emission wavelength (*34*). All absorbance measurements were performed using a JASCO V-630 spectrophotometer.

Association Kinetics. The kinetics of association of plumbagin with tubulin was measured under pseudo-first-order reactions (where the ligand was present in a large excess) (*35, 36*). Tubulin concentration was 1 μM in all cases, and the plumbagin concentrations were 20 μM, 30 μM and 40 μM in three sets of rate constant measurements. The ligand was added to tubulin solution, and emission at 335 nm was measured upon excitation at 295 nm with time at 25 °C using 5 nm excitation and 10 nm emission slits. The quenching data were analyzed according to the methods of Lambier and Engelborghs (*37*) and others (*35, 36*) after correction of the inner filter effect.

$$F = Ae^{-k_1 t} + Be^{-k_2 t} + C \quad (3)$$

where F is the fluorescence of the ligand−tubulin complex at time t, A and B are the amplitudes for the fast and slow phases, k_1 and k_2 are the pseudo-first-order rate constants for the fast and the slow phases, respectively, and C is an integration constant. The data were analyzed by Microcal Origin version 7.0 software. The apparent second-order rate constants for fast and slow phases were obtained by dividing the observed rate constant for the fast phase (k_1) and slow phase (k_2) by the ligand concentration.

Job Plot. The stoichiometry of binding was determined using the method of continuous variation (*38, 39*). Several mixtures of tubulin and plumbagin were prepared by continuously varying concentrations of tubulin and plumbagin in the mixture keeping the total concentration of plumbagin plus tubulin constant at 5 μM. Reaction mixtures were incubated at 25 °C for 60 min, and the quenching of tryptophan fluorescence was recorded at 335 nm.

Dissociation Constant (K_d). Tubulin (2 μM) was incubated with varying concentrations of plumbagin (0−30 μM) at 25 °C for 60 min. The fluorescence intensity was measured at 335 nm upon excitation at 295 nm. The apparent decrease in the fluorescence values in the presence of varying concentrations of plumbagin were corrected for the inner filter effect. The fraction of binding sites (X) occupied by plumbagin was determined using an equation $X = (F_0 - F)/F_{max}$, where F_0 is the fluorescence intensity of tubulin in the absence of plumbagin, F is the corrected fluorescence intensity of tubulin in the presence of plumbagin, and F_{max} is calculated from the plot of $1/(F_0 - F)$ versus 1/[plumbagin] and extrapolating 1/[plumbagin] to zero as shown in Figure 7B. The dissociation constant (K_d) was determined using the relationship (*29, 40*)

$$F_{max}/(F_0 - F) = 1 + K_d/L_f \quad (4)$$

where L_f represents free plumbagin concentration; $L_f = C - X[Y]$, where C is the total concentration of plumbagin and [Y] is the molar concentration of ligand-binding sites using a stoichiometry of 1:1 as determined from the Job plot.

Modified Dixon Plot. A modified Dixon plot for plumbagin−tubulin binding was obtained using colchicine as a competitive inhibitor. Colchicine binding to tubulin in the presence of plumbagin was determined by measuring the fluorescence of tubulin−colchicine complex (*41*). The reaction mixtures containing tubulin (3 μM) and a range of concentrations of colchicine (5−15 μM) and plumbagin (0−50 μM) were incubated at 37 °C for 45 min. The reciprocal of the fluorescence intensity of the colchicine tubulin complex at 430 nm was plotted against the concentration of the plumbagin. The resulting Dixon plot gave an approximate K_i value for the plumbagin (*41*).

Statistical Analysis. Data are presented as the mean of at least three independent experiments along with SEM. Statistical analysis of data was done by Student's t test, by using MS Excel, and two measurements were statistically significant if the corresponding p value was <0.05.

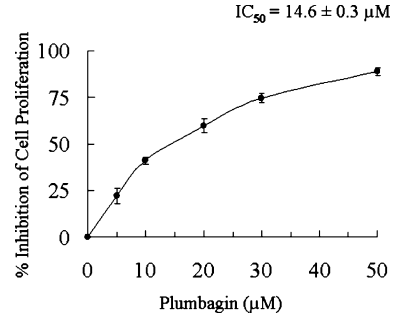

FIGURE 2: Concentration-dependent inhibition of cell proliferation (MTT assay). Results of MTT assay of (0−50 μM) plumbagin-treated A549 cells. Details of the experiment are given in Experimental Procedures.

RESULTS AND DISCUSSION

Plumbagin Inhibits Cell Proliferation of A549 Cells. Plumbagin is known to inhibit cell proliferation with IC_{50} value of 11.7 μM for human non-small lung cancer (A549) cells (*10*). Using the same cell line (A549) we have reproduced these results under our experimental conditions. Plumbagin inhibited cell proliferation in A549 cancer cell lines in a concentration-dependent manner as measured by MTT assay (Figure 2) (explained in Experimental Procedures). Maximal proliferation inhibition observed was 84.6% at 12 h with 50 μM plumbagin, with calculated IC_{50} value of 14.6 ± 0.3 μM. Therefore, our result corroborated well with previously reported value (*10*).

Alteration in Cellular Morphology of A549 Cells by Plumbagin. Plumbagin has been shown to arrest cell cycle at G2/M phase and induce apoptosis in a number of cell lines (*10, 12*). We were interested to see the effect of plumbagin on cellular morphology of human non-small cell lung cancer cells (A549). Lung epithelium carcinoma (A549)

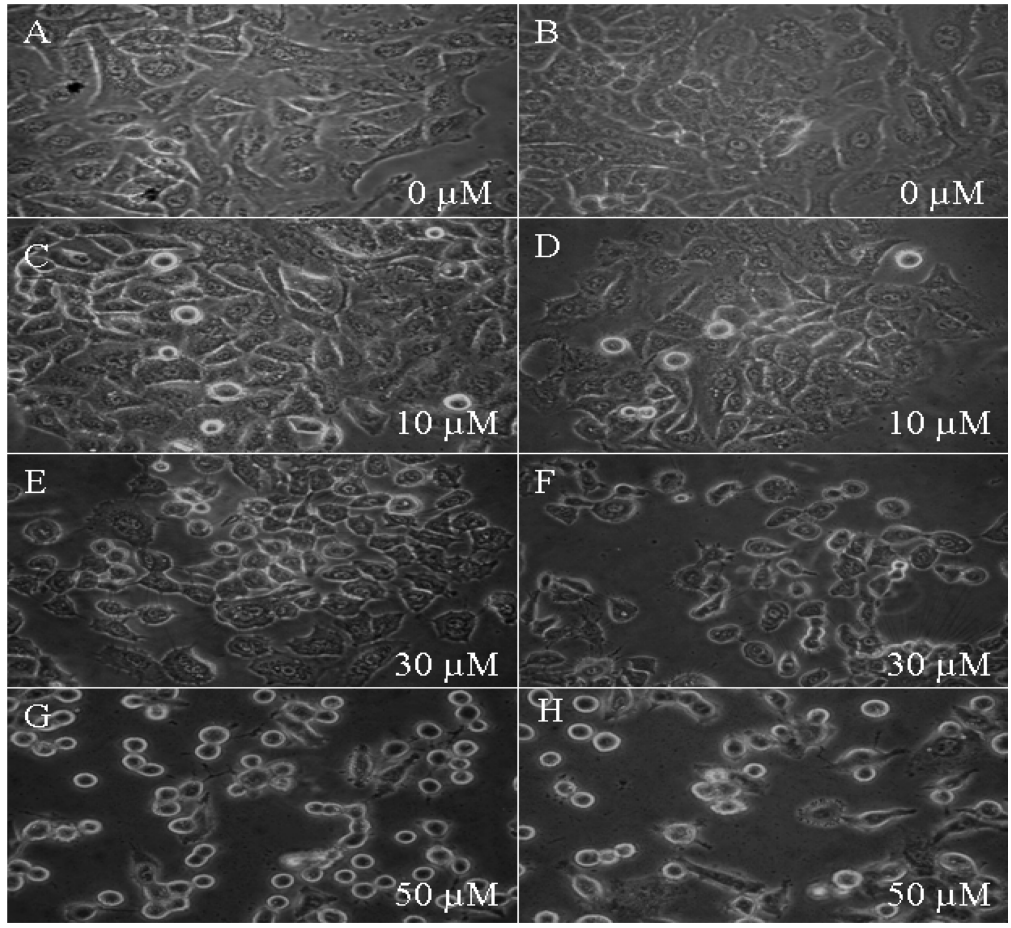

FIGURE 3: Bright field images of the plumbagin treated A459 cells were taken by Olympus inverted microscope model CKX41. Effects of plumbagin (0−50 μM) on cellular architecture of A549 cells in 3 h [A−H] are shown.

cells were incubated in the presence of varying concentrations of plumbagin (0−50 μM) for 3 h. Aberrations in the cellular morphology such as contraction and shrinkage were observed (Figure 3). Bright field images of the treated cells were taken by Olympus inverted microscope model CKX41. Below 10 μM concentration of plumbagin, there was no significant change in the morphology of the cells. Cell shapes started changing above 10 μM plumbagin, and the cells became smaller in size and more round-shaped at and above 50 μM (Figure 3). These results clearly indicated that plumbagin is responsible for the altered morphology of A549 cells.

Disruption of Interphase Microtubule Network of A549 Cells by Plumbagin. The tubulin−microtubule system plays a major role to maintain cellular morphology. Because plumbagin effectively altered the morphology of A549 cells (Figure 3), we were interested to know whether plumbagin targets the microtubule network in A549 cultured cells. This was examined by confocal microscopy (Figure 4). Control A549 cells showed typical interphase microtubule organization. No effect of plumbagin on the interphase microtubule network was apparent at concentrations below 10 μM. However, at higher plumbagin concentrations (30 μM), a significant reduction of microtubule density occurred. This reduction in the number of microtubules at the periphery of the cells was apparent with disorganized central networks. Plumbagin strongly disrupted interphase microtubule in A549 cells at 50 μM concentration, and these results indicated that plumbagin may also perturb microtubule dynamics. Several microtubule inhibitors have been shown to suppress microtubule dynamics strongly (*23–30*).

Inhibition of Microtubule Polymerization by Plumbagin in Vitro. Since plumbagin affects the cellular architecture of cells by perturbing the intercellular microtubular network, the effect of plumbagin on microtubule polymerization was examined using purified tubulin by light scattering assay (as explained in Experimental Procedures). Purified tubulin (12 μM) was polymerized in the absence or presence of different concentrations of plumbagin, and the results of such experiments are shown in Figure 5A. Plumbagin inhibited the rate and the extent of tubulin polymerization in a concentration-dependent manner (Figure 5A). Thus, the inhibition of polymerization was 68% when 85 μM plumbagin was used, and 50% inhibition of microtubule polymerization (IC_{50}) occurred at plumbagin concentration of 38.5 $\pm$ 0.5 μM ($P < 0.01$).

This inhibition of the tubulin polymerization, in the presence of plumbagin, as observed by light scattering assay, could be due to the formation of very short microtubules, altered polymer morphology or formation of small aggregates of tubulin. To distinguish among these possibilities, polymers formed in the presence of plumbagin were examined by electron microscopy. Consistent with previous reports (*31*) tubulin polymerized in the presence of 1 M glutamate formed mainly open sheets of parallel protofilaments (Figures 5B). In the presence of 30 μM plumbagin, peeling of protofilaments was observed and large protofilaments were frag-

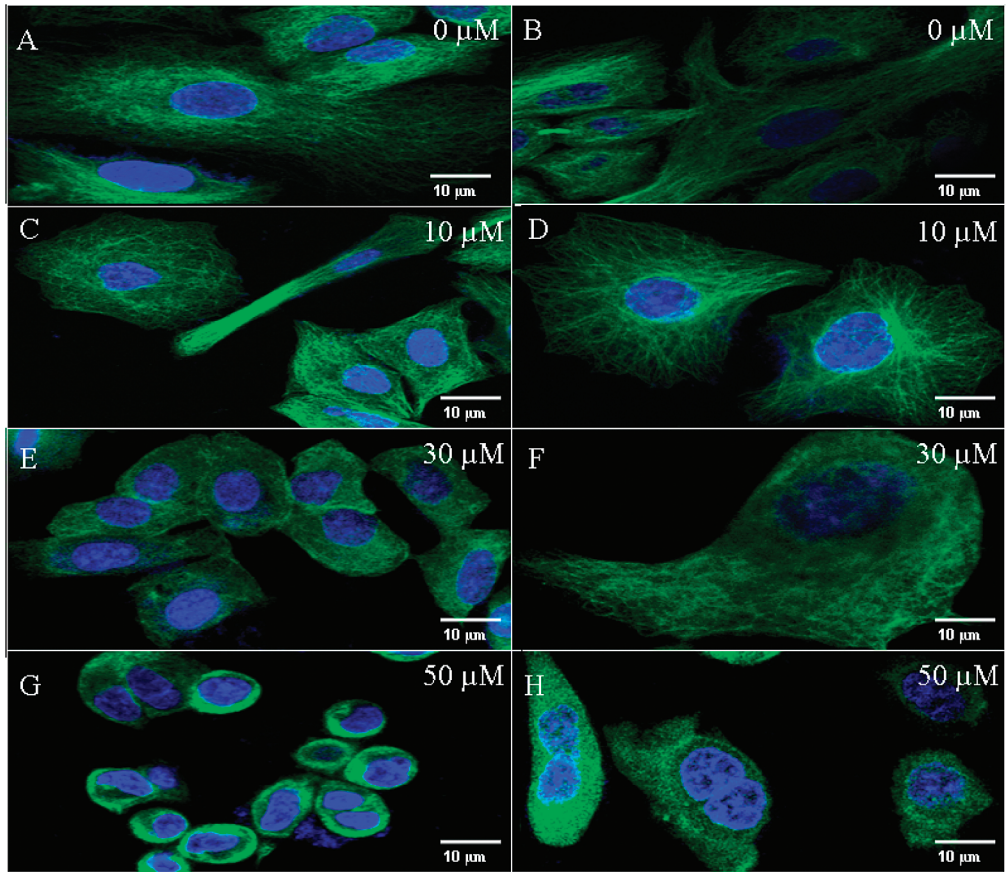

FIGURE 4: Immunofluorescence study of interphase microtubule depolymerization of A549 cells by plumbagin. Effects of (0−50) μM plumbagin on microtubule networks of A549 cells in different fields as shown in panels [A−H]. Control indicates solvent (0 0.1% DMSO) treated cells. Microtubule is tagged by FITC (green), and nucleus is tagged by DAPI (blue).

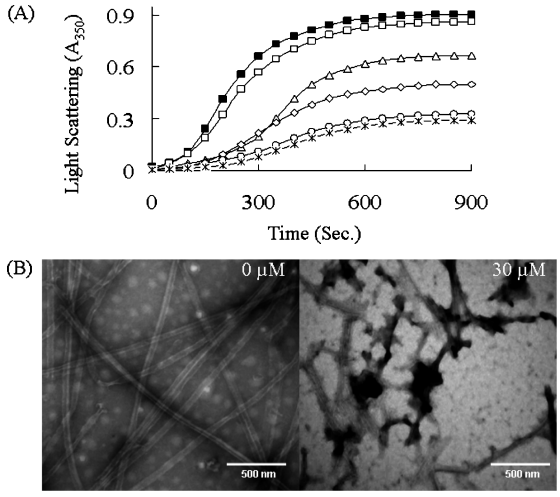

FIGURE 5: Effect of plumbagin on tubulin polymerization. (A) Tubulin (12 μM) was mixed with plumbagin at different concentrations as follows: 0 (■), 15 (□), 25 (△), 35(◇), 50 (○), and 85 (∗) μM at 37 °C in PEM buffer and assembly reaction monitored for the indicated period 37 °C. (B) Microtubules in the absence (left panel) and presence of 30 μM plumbagin (right panel) as visualized by electron microscopy. Images were taken at 63000× magnification. Details of the polymerization reaction and electron microscopy are explained in Experimental Procedures.

mented into small protofilaments with respect to the control microtubular structure.

Plumbagin Binding to Tubulin. The binding of plumbagin to tubulin has been studied by measuring the quenching of the intrinsic tryptophan fluorescence of tubulin. Plumbagin quenches the intrinsic tryptophan fluorescence of tubulin in a time- and concentration-dependent manner. Addition of 40 μM plumbagin to tubulin (1 μM) quenches about 80% of its tryptophan fluorescence during 60 min incubation at 25 °C (Figure 6A). Without incubation quenching was about 15% when plumbagin was added to tubulin. Increase of tryptophan quenching with time indicates time-dependent binding at 25 °C, which took about 60 min for completion. Similar results were observed when colchicine was added to tubulin (data not shown). Plumbagin did not alter the λ_{max} of the tryptophan emission wavelength of tubulin, suggesting that the binding of plumbagin did not alter the polarity of the immediate environment of tryptophan residues in tubulin.

The association rate constants of tubulin−plumbagin interactions were determined using different concentrations of plumbagin (20 μM, 30 μM, and 40 μM) with 1 μM tubulin by ligand-induced quenching of tubulin fluorescence. Figure 6A shows the time course of the quenching of tryptophan fluorescence upon plumbagin binding to tubulin under pseudo-first-order conditions. The logarithmic plot in Figure 6B shows the presence of two phases when analyzed according to the method of Lambier and Engelborghs (*37*) and others (*35, 36*) as explained in Experimental Procedures. Apparent second-order rate constants for the fast phase and slow phase have been found to be 235.12 ± 36 M^{-1} s^{-1} and 11.63 ± 11 M^{-1} s^{-1} at 25 °C respectively taking the average of nine determinants using three different concentrations of plumbagin. Under the same experimental conditions and analysis, the apparent second-order rate constants of colchicine binding to tubulin were similar to previously reported

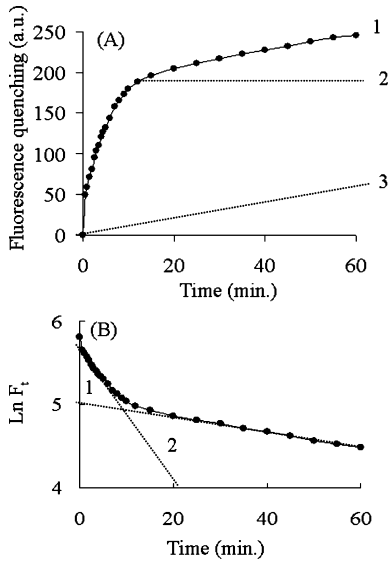

FIGURE 6: Kinetics of plumbagin binding to tubulin. (A) Quenching of tryptophan fluorescence of tubulin upon binding of plumbagin to tubulin. Tubulin (1 μM) in PEM buffer was mixed with 40 μM plumbagin. Kinetics was followed for 60 min at 25 °C by measuring the intensity of intrinsic protein fluorescence at 335 nm upon excitation at 295 nm. Trace 1, overall quenching of tryptophan quenching; trace 2, fast phase; trace 3, slow phase as determined by the analysis described in Experimental Procedures. (B) The semilogarithmic plot of ln F_t versus time. The biphasic plot obtained was resolved into its component phases as described in the Experimental Procedures. The fast and slow phases are shown in 2 and 1 respectively. Data are represented as mean ± SEM ($P < 0.01$) where ($n = 3$).

values (data not shown) (*42*). It is established that the biphasic nature of the colchicine−tubulin interaction arises due to differential binding property of colchicine to β-tubulin-isotypes present in brain tubulin (*42–44*). Colchicine and plumbagin are structurally unrelated. Nevertheless, both ligands recognize and differentiate the colchicine binding site of β-tubulin in a similar way.

The stoichiometry and the dissociation constant (K_d) of the tubulin−plumbagin interaction have been estimated by measuring the tryptophan quenching of tubulin upon plumbagin binding. Stoichiometry of the ligand−protein complex was determined using the Job plot. In this plot, concentrations of both tubulin and plumbagin were varied keeping the total drug−protein concentration fixed at 5 μM. Results of such experiments are shown in Figure 7A. The stoichiometry of binding, calculated by using this method of continuous variation (*38, 39*), was found to be 1:1.

The dissociation constant was estimated from Figures 7B and 7C. Figure 7B shows the quenching profile of a fixed amount of tubulin (2 μM) with various concentrations of plumbagin (0−30 μM). All fluorescence data were corrected for the inner filter effect. Either the dissociation constant (K_d) or the stoichiometry can be obtained from such plots if the other is known. We determined the dissociation constant (K_d) as the stoichiometry was already determined as 1:1. Details of the binding data analysis have been described in the Experimental Procedures, and the analysis of the data yielded a linear plot (Figure 7C) with a dissociation constant of 0.936 ± 0.71 μM ($P < 0.01$).

Plumbagin Binds Tubulin Competitively at the Colchicine Binding Site. Many structurally unrelated natural and synthetic compounds that inhibit microtubule polymerization bind to the colchicine-binding site of tubulin (*25*). Like colchicine, plumbagin also inhibited tubulin polymerization. Thus, we examined whether plumbagin binds at the colchicine binding site of tubulin. Colchicine does not fluoresce in aqueous solution, but it fluoresces when bound to tubulin (*45*). Tubulin was incubated with a fixed concentration of colchicine and different concentration of plumbagin (0−30 μM), and the fluorescence of colchicine of different samples was measured. Plumbagin inhibited colchicine binding to tubulin in a concentration-dependent manner. The data were analyzed using a modified Dixon plot (Figure 8A). The results clearly indicate that binding of plumbagin to tubulin is competitively inhibited by colchicine, yielding a K_i value of 7.5 μM.

One of the important characteristics of colchicine binding to tubulin is its irreversibility. This property of the drug−protein interaction has been found to be associated with colchicine structure, especially its B-ring side chain. Although plumbagin, an inhibitor for the drug colchicine, bears significant similarity with the colchicine−tubulin interaction, its structure is unrelated with colchicine. To determine the reversibility of the plumbagin−tubulin interaction, plumbagin (15 μM) was incubated with tubulin at 25 °C (*46*). At different time intervals, aliquots of drug−protein complex were withdrawn and the extent of free colchicine binding site of tubulin was estimated by adding a colchicine analogue AC (2-methoxy-5-(2′,3′,4′-trimethoxyphenyl)-tropone), which binds tubulin instantaneously at the colchicine site and emits fluorescence with λ_{max} at 430 nm. Results of such an experiment where fluorescence of AC was measured at 430 nm are shown in Figure 8B. The results indicate that the fluorescence of AC decreases with increasing incubation time of the tubulin−plumbagin complex at 25 °C. Here, the fluorescence of the AC−tubulin complex without plumbagin was considered as 100% (control) and the fluorescence of the tubulin−plumbagin complex incubated for 10 min at 25 °C was found to be 80% of the control value. Fluorescence of the complex decreased further to 42% when the complex was incubated for 60 min. The experimental data clearly indicate that the nature of interaction of plumbagin with tubulin is irreversible.

In the present study the antiproliferative activity of plumbagin has been correlated to its ability to disrupt microtubule polymerization through tubulin binding. Plumbagin is structurally unrelated to colchicine, yet it binds tubulin at the colchicine site. Like colchicine, its binds slowly, requiring about 60 min at 25 °C for equilibration. The values of the rate constants are comparable to that of colchicine. The stoichiometry of binding is one mole of ligand per mole of tubulin. The K_d value is around 1 μM. Like colchicine binding to tubulin, plumbagin binds irreversibly. The IC_{50} value of plumbagin of cells in culture is 1000-fold higher than popular antimitotic agents like paclitaxel, colchicine and vinblastine (*47*). The reason for the higher IC_{50} value of plumbagin of cells in culture is not known. One possibility is that the local concentration of plumbagin inside cells for reaction with tubulin−microtubule is low. This may be due to the fact that plumbagin has many other activities in cells (*6–13, 48*). Many natural compounds like curcumin, sanguinarine, quercetin and verapamil have antimitotic activities with higher IC_{50} values (comparable with plumbagin) of cells in culture, and these compounds also have many other activities in cells (*26, 49, 50*). Antimitotic compounds commonly perturb

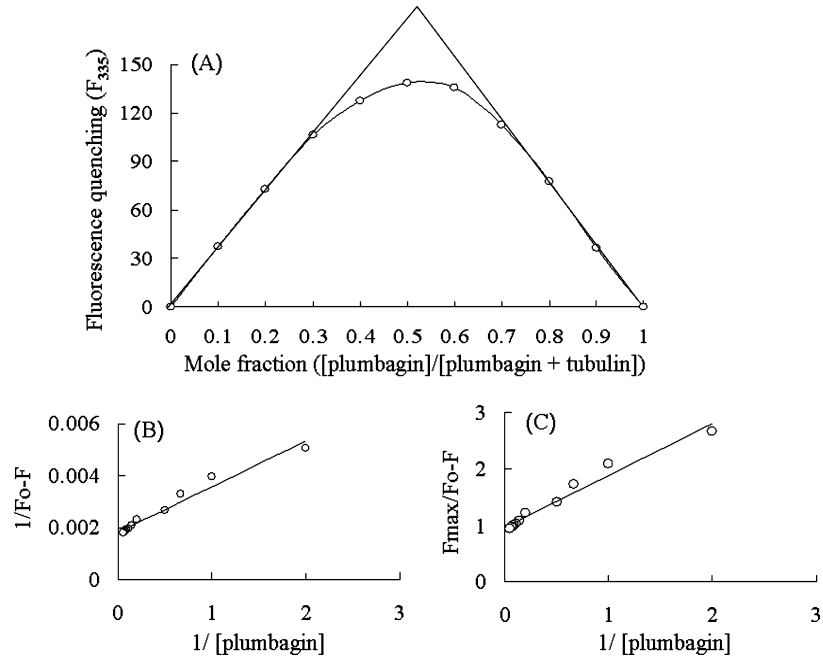

FIGURE 7: Characterization of plumbagin binding to tubulin. (A) Job's plot of plumbagin binding to tubulin. The concentrations of tubulin and plumbagin were varied continuously, keeping the total concentration of plumbagin plus tubulin constant at 5 μM. The corrected fluorescence intensities at 335 nm were plotted against the mole fractions of plumbagin. Data are represented as mean ± SEM ($P < 0.01$) where $n = 3$. (B) Double reciprocal plot of plumbagin binding to tubulin. F_{max} has been determined from the $1/(F_0 - F)$ and 1/[plumbagin] graph. (C) The linear plot of binding of plumbagin to tubulin. Data are represented as mean ± SEM ($P < 0.01$) where $n = 3$. Data are representative of three identical experiments.

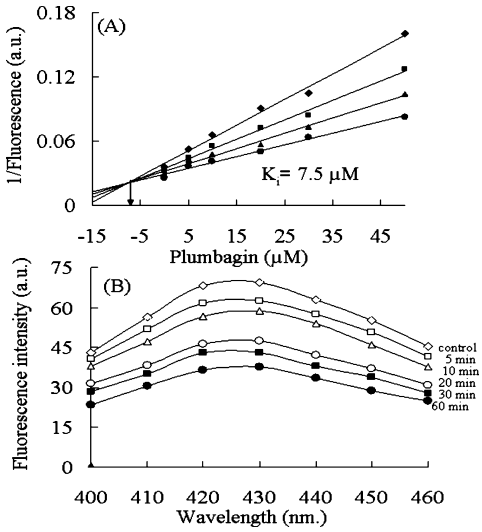

FIGURE 8: Plumbagin inhibited the binding of colchicine to tubulin. (A) Modified Dixon plot. The concentrations of colchicine were 5 μM (◆), 7.5 μM (■), 10 μM (△) and 15 μM (●) respectively. The reaction mixture contained tubulin (3 μM) and plumbagin at the indicated concentration (5−50 μM), and they were incubated at 37 °C for 1 h. Data are represented as mean ± SEM ($P < 0.01$) where $n = 3$. (B) Reversible binding study. Tubulin 3 μM was incubated with plumbagin (15 μM) for different time intervals, 0 min (◇), 5 min (□), 10 min (△), 20 min (○), 30 min (■) and 60 min (●), and then 30 μM AC was added in the sample separately. Fluorescence spectra were taken when the excitation wavelength was 370 nm.

mitotic spindle function by interfering with microtubule dynamics, and this effect is reflected in their abilities to modulate the polymerization of microtubules *in vitro*. Inhibition of polymerization of tubulin into microtubules by plumbagin suggests that it may interfere with the microtubule dynamics also. There are three distinct antimitotic drug binding sites in tubulin which are targeted for the anticancer drug developments. Although no drug has been developed yet for targeting the colchicine binding site, there are few drugs which are in the advance stage of clinical trails. Paclitaxel is most successful among anticancer drugs currently used in chemotherapy. However, currently available antimitotic drugs suffer from the problem of multidrug resistance. Another limitation of these drugs is their specificity toward a particular type of tumor. Therefore there is a need to develop a large numbers of drugs and their analogues, with and without structural similarity and variations of substituents against a particular drug binding site. A large pool of drugs is also essential from the point of view of drug design. For this purpose, further research is necessary to establish pharmacophoric points of attachment of plumbagin at the colchicine binding site.

ACKNOWLEDGMENT

The authors wish to thank Prof. Gautam Basu, Department of Biophysics, Bose Institute, Kolkata, India, for critical reading and suggestions for preparation of the manuscript. The authors also wish to thank Mr. Sailen Dey, Indian Institute of Chemical Biology, Kolkata, India, for technical assistance during EM study.

REFERENCES

1. Van der Vijver, L. M. (1972) Distribution of plumbagin in the Plumbaginaceae. *Phytochemistry 11*, 3247–3248.
2. Mossa, J. S., El-Feraly, F. S., and Muhammad, I. (2004) Antimycobacterial constituents from Juniperus procera, Ferula communis and Plumbago zeylanica and their in vitro synergistic activity with isonicotinic acid hydrazide. *Phytother. Res. 18*, 934–937.
3. Likhitwitayawuid, K., Kaewamatawong, R., Ruangrungsi, N., and Krungkrai, J. (1998) Antimalarial naphthoquinones from Nepenthes thorelii. *Planta Med. 64* (3), 237–241.
4. de Paiva, S. R., Figueiredo, M. R., Aragão, T. V., and Kaplan, M. A. C. (2003) Antimicrobial Activity in Vitro of Plumbagin Isolated from *Plumbago S*pecies. *Mem. Inst. Oswaldo Cruz 98* (7), 959–961.

5. Tilak, J. C., Adhikari, S., and Devasagayam, T. P. (2004) Antioxidant properties of *Plumbago zeylanica*, an Indian medicinal plant and its active ingredient, plumbagin. *Redox Rep. 9*, 219–227.
6. Hazra, B., Sarkar, R., Bhattacharyya, S., Ghosh, P. K., Chel, G., and Dinda, B. (2002) Synthesis of plumbagin derivatives and their inhibitory activities against Ehrlich ascites carcinoma in vivo and *Leishmania donovani* promastigotes *in vitro*. *Phytother. Res. 16*, 133–137.
7. Sugie, S., Okamoto, K., and Rahman, K. M. (1998) Inhibitory effects of plumbagin and juglone on azoxymethane-induced intestinal carcinogenesis in rats. *Cancer Lett. 127*, 177–183.
8. Srinivas, G., Annab, L. A., Gopinath, G., Banerji, A., and Srinivas, P. (2004) Antisense blocking of BRCA1 enhances sensitivity to plumbagin but not tamoxifen in BG-1 ovarian cancer cells. *Mol. Carcinog. 39*, 15–25.
9. Singh, U. V., and Udupa, N. (1997) Reduced toxicity and enhanced antitumor efficacy of betacyclodextrin plumbagin inclusion complex in mice bearing Ehrlich ascites carcinoma. *Indian J. Physiol. Pharmacol. 41*, 171–175.
10. Hsu, Y.-L., Cho, C.-Y., Kuo, P.-L., Huang, Y.-T., and Lin, C.-C. (2006) Plumbagin (5-Hydroxy-2-methyl-1,4-naphthoquinone) Induces Apoptosis and Cell Cycle Arrest in A549 Cells through p53 Accumulation via c-Jun NH2-Terminal Kinase-Mediated Phosphorylation at Serine 15 in Vitro and in Vivo. *J. Pharmacol. Exp. Ther. 318*, 484–494.
11. Zhao, Y. L., and Lu, D. P. (2006) Effects of plumbagin on the human acute promyelocytic leukemia cells in vitro. *J. Exp. Hematol. 14* (2), 208–211.
12. Kuo, P.-L., Hsu, Y.-L., and Cho, C.-Y. (2006) Plumbagin induces G2-M arrest and autophagy by inhibiting the AKT/mammalian target of rapamycin pathway in breast cancer cells. *Mol. Cancer Ther. 5* (12), 3209–3221.
13. Sandur, S. K., Ichikawa, H., Sethi, G., Ahn, K. S. , and Aggarwal, B. B. (2006) Plumbagin (5-Hydroxy-2-methyl-1,4-naphthoquinone) Suppresses NFκB Activation and NFκB regulated Gene Products Through Modulation of p65 and IκBα Kinase Activation, Leading to Potentiation of Apoptosis Induced by Cytokine and Chemotherapeutic Agents. *J. Biol. Chem. 281* (25), 17023–17033.
14. Nogales, E., Whittaker, M., Milligan, R. A., and Downing, K. H. (1999) High-resolution model of the microtubule. *Cell 96*, 79–88.
15. Desai, A., and Mitchison, T. J. (1997) Microtubule polymerization dynamics. *Annu. Rev. Cell. Dev. Biol. 13*, 83–117.
16. Zhou, J., Yao, J., and Joshi, H. C. (2002) Attachment and tension in the spindle assembly checkpoint. *J. Cell Sci. 115*, 3547–3555.
17. Hoffman, D. B., Pearson, C. G., Yen, T. J., Howell, B. J., and Salmon, E. D. (2001) Microtubule-dependent changes in assembly of microtubule motor proteins and mitotic spindle checkpoint proteins at PtK1 kinetochores. *Mol. Biol. Cell. 12* 1995–2009.
18. Wilson, L., Panda, D., and Jordan, M. A. (1999) Modulation of microtubule dynamics by drugs: A paradigm for the actions of cellular regulators. *Cell Struct. Funct. 24*, 329–335.
19. Jordan, M. A., and Wilson, L. (2004) Microtubules as a target for anticancer drugs. *Nat. Rev. Cancer. 4*, 253–265.
20. Hamel, E. (1996) Antimitotic natural products and their interactions with tubulin. *Med. Res. Rev. 16*, 207–231.
21. Jordan, M. A. (2002) Mechanism of action of antitumor drugs that interacts with microtubules and tubulin. *Curr. Med. Chem.-Anti-Cancer Agents 2*, 1–17.
22. Holmes, F. A., Walters, R. S., Theriault, R. L., Forman, A. D., Newton, L. K., Raber, M. N., Buzdar, A. U., Frye, D. K., and Hortobagyi, G. N. (1991) Phase II trial of taxol, an active drug in the treatment of metastatic breast cancer. *J. Natl. Cancer Inst. 83*, 1797–1805.
23. Schiller, J. H., Harring, D., Belani, C. P., Langer, C., Sandler, A., Krook, J., and John, D. H. (2002) Comparison of four chemotherapy regiments for advanced non-small-cell lung cancer. *N. Engl. J. Med. 346*, 92–98.
24. Cowden, C. J., and Paterson, I. (1997) Synthetic chemistry Cancer drugs better than Taxol? *Nature 387*, 238–239.
25. Bhattacharyya, B., Panda, D., Gupta, S., and Banerjee, M. (2008) Anti-mitotic activity of colchicine and the structural basis for its interaction with tubulin. *Med. Res. Rev. 28* (1), 155–183.
26. Gupta, K. K., Bharne, S. S., Rathinasamy, K., Naik, N. R., and Panda, D. (2006) Dietary antioxidant curcumin inhibits microtubule assembly through tubulin binding. *FEBS J. 273* 5320–5332.
27. Prager-Khoutorsky, M., Goncharov, I., Rabinkov, A., Mirelman, D., Geiger, B., and Bershadsky, A. D. (2007) Allicin inhibits cell polarization, migration and division via its direct effect on microtubules. *Cell Motil. Cytoskeleton 64*, 321–337.
28. Panda, D., Rathinasamy, K., Santra, M. K., and Wilson, L. (2005) Kinetic suppression of microtubule dynamic instability by griseofulvin: implications for its possible use in the treatment of cancer. *Proc. Natl. Acad. Sci. U.S.A. 102*, 9878–9883.
29. Gupta, K., and Panda, D. (2002) Perturbation of microtubule polymerization by quercetin through tubulin binding: a novel mechanism of its antiproliferative activity. *Biochemistry 41*, 13029–13038.
30. Gupta, K., Bishop, J., Peck, A., Brown, J., Wilson, L., and Panda, D. (2004) Antimitotic antifungal compound benomyl inhibits brain microtubule polymerization and dynamics and cancer cell proliferation at mitosis, by binding to a novel site in tubulin. *Biochemistry 43*, 6645–6655.
31. Hamel, E., and Lin, C. M. (1981) Glutamate-induced polymerization of tubulin: characteristics of the reaction and application to the large-scale purification of tubulin. *Arch. Biochem. Biophys. 209*, 29–40.
32. Bradford, M. M. (1976) A rapid and sensitive method for the quantitation of microgram quantities of protein utilizing the principle of protein-dye binding. *Anal. Biochem. 72*, 248–254.
33. Gaskin, F., Cantor, C. R., and Shelanski, M. L. (1974) Turbidimetric studies of the in vitro assembly and disassembly of porcine neurotubules. *J. Mol. Biol. 89*, 737–755.
34. Lakowicz, J. R. (1999) *Principles of Fluorescence Spectroscopy*, 2nd ed., Kluwer Academic/Plenum Publishers, New York.
35. Chakrabarti, G., Sengupta, G., and Bhattacharyya, G. (1996) Thermodynamics of Colchicinoid-Tubulin Interactions role of B ring and C7 substituent. *J. Biol. Chem. 271*, 2897–2901.
36. Pyles, A. E., and Bane, S. H. (1993) Effect of the B ring and the C-7 substituent on the kinetics of colchicinoid-tubulin associations. *Biochemistry 32*, 2329–2336.
37. Lambeir, A., and Engelborghs, Y. (1981) A fluorescence stopped flow study of colchicine binding to tubulin. *J. Biol. Chem. 256*, 3279–3282.
38. Huang, C. Y. (1982) Determination of binding stoichiometry by the continuous variation method: the Job plot. *Methods Enzymol. 87*, 509–525.
39. Ward, L. D. (1985) Measurement of ligand binding to protein by fluorescence spectroscopy. *Methods Enzymol. 117*, 400–414.
40. George, C. Na., and Timasheff, S. N. (1986) Interaction of vinblastine with calf brain tubulin: multiple equilibria. *Biochemistry 25*, 6214–6222.
41. Chakraborty, S., Gupta, S., and Bhattacharyya, B. (2004) The B-ring substituent at C-7 of colchicine and the α-C-terminus of tubulin communicate through the "tail-body". *Proteins 57* (3), 602–609.
42. Gupta, S., Banerjee, M., Poddar, A., Banerjee, A., Basu, G., Roy, D., and Bhattacharyya, B. (2005) Biphasic Kinetics of the Colchicine-Tubulin Interaction: Role of Amino Acids Surrounding the A ring of Bound Colchicine Molecule. *Biochemistry 44*, 10181–10188.
43. Banerjee, A., and Luduena, R. F. (1987) Kinetics of association and dissociation of colchicine-tubulin complex from brain and renal tubulin. Evidence for the existence of multiple isotypes of tubulin in brain with differential affinity to colchicine. *FEBS Lett. 219*, 103–107.
44. Banerjee, A., and Luduena, R. F. (1992) Kinetics of colchicine binding to purified β-tubulin isotypes from bovine brain. *J. Biol. Chem. 267*, 13335–13339.
45. Bhattacharyya, B., and Wolff, J. (1974) Promotion of fluorescence upon binding of colchicine to tubulin. *Proc. Natl. Acad. Sci. U.S.A. 71*, 2627–2631.
46. Gupta, S., Das, L., Datta, A. B., Poddar, A., Janik, M. E., and Bhattacharyya, B. (2006) Oxalone and Lactone Moieties of Podophyllotoxin Exhibit Properties of Both the B and C Rings of Colchicine in Its Binding with Tubulin. *Biochemistry 45*, 6467–6475.
47. Martelleo, A. L., McDavid, M. H., and Horwitz, B. S. (2000) Taxol and Discodermolide represent a synergistic drug combination in Human carcinoma cell lines. *Clin. Cancer Res. 6* 1978–1987.
48. Wang, C. C., Chiang, Y. M., Sung, S. C., Hsu, Y. L., Chang, J. K., and Kuo, P. L. (2008) Plumbagin induces cell cycle arrest and apoptosis through reactive oxygen species/c-Jun N-terminal kinase pathways in human melanoma A375.S2 cells. *Cancer Lett. 259*, 82–98.
49. Lopus, M., and Panda, D. (2006) The benzophenanthridine alkaloid sanguinarine perturbs microtubule assembly dynamics through tubulin binding,A possible mechanism for its antiproliferative activity. *FEBS J. 273*, 2135–2150.
50. Yanq, J. H., Hsia, T. C., and Chunq, J. G. (2006) Inhibition of lung cancer cell growth by quercetin glucuronides via G2/M arrest and induction of apoptosis. *Drug Metab. Dispos. 34* (2), 296–304.

BI800730Q